

Synthesis and Dynamic Rheological Behavior of Polybutadiene Star Polymers

C. H. Adams,[†] L. R. Hutchings,[†] P. G. Klein,^{*,‡} T. C. B. McLeish,[†] and R. W. Richards^{*,†}

IRC Polymer Science and Technology, University of Durham, Durham DH1 3LE, U.K., and University of Leeds, Leeds LS2 9JT, U.K.

Received December 26, 1995; Revised Manuscript Received April 30, 1996[®]

ABSTRACT: Polybutadiene star polymers, of nominal functionality 3, 4, 8 and 12, all with arm lengths of approximately 30 000 g mol⁻¹, have been synthesized using chlorosilane coupling agents. Dynamic mechanical studies have been carried out using parallel-plate rheometry at various temperatures, and the data frequency–temperature shifted to produce master curves. Fits to the Ball–McLeish constraint release theory indicate an effective entanglement molecular weight somewhat higher than the literature value for a linear polymer. This has been interpreted by considering a dilution of constraints effect caused by the Rouse diffusion of the terminal section of the star arm, leading to a predicted modified entanglement molecular weight similar to that found experimentally. Evidence for the Rouse-like behavior of the terminal section has been obtained from deuterium NMR spectra of a selectively deuterated sample. The presence of small amounts of residual linear chains is shown to be responsible for a further dilution of entanglements. An extension of the theoretical fits to include the high-frequency Rouse mode spectrum shows a divergence between theory and experiment which is indicative of the onset of the glass transition.

Introduction

The dynamics of entangled polymers is currently understood within the framework of the tube model.¹ In the case of linear chains, the effective constraints due to neighboring molecules restrict the long-time motion of a given molecule to curvilinear diffusion along its own contour, a dynamical mode termed “reptation”. The molecule behaves as if it were trapped in a tube which is itself a coarse-grained representation of the molecular path.

Molecules of branched topology are still subject to the tube-like constraints, but must undergo different dynamics to change their configurations, because reptation is suppressed by the branch points. The simplest example is the star polymer, which has been the subject of extensive theoretical and experimental studies.^{2–5} We discuss here an examination of a dynamical theory of star polymers (the Ball–McLeish⁴ model) using rheological data on a series of star polybutadienes. These star polymers have monodisperse arm molecular weights of approximately 30 000 g mol⁻¹ and are of well-defined functionality ranging from 3 to 12. Additionally, the molecular dynamics of the terminal entanglement length of a 4-arm star are investigated using deuterium NMR, and the dynamics of this terminal section are shown to have significant consequences for the interpretation of the rheology according to the model.

A précis of the relevant theoretical background is given below. This is followed by an experimental section where the synthetic, rheological, and NMR methods are detailed. Finally, we discuss the results of the dynamic rheology experiments and compare them to the theoretical predictions.

Theoretical Background

As discussed above, reptation is not possible for star polymers, and instead the configurational relaxations

are now controlled by fluctuations of the entangled tube length in which the free end of the star arm retraces some of its tube before a further outward exploration of the melt. This motion completely renews the configuration of the outer part of the arm as far as the deepest retraction. However, the deeper the retraction, the more unlikely its occurrence, since deeper retractions correspond to exponentially fewer configurational states of the molecule. In consequence, each tube segment, or entanglement length, of the star arm has its own characteristic relaxation time, which depends on its distance from the free end. Following the theoretical model of Ball and McLeish,⁴ this relaxation time is given by eq 1.

$$\tau_{(x)} = \tau_0 \exp \left[2\nu \left(\frac{M_a}{M_e} \right) \left(\frac{x^2}{2} - \frac{x^3}{3} \right) \right] \quad (1)$$

where $\tau_{(x)}$ is the relaxation time of an entanglement length a fractional distance x from the free end of the arm, M_a the arm molecular weight, M_e the entanglement molecular weight, and ν a constant equal to ¹⁵/₈. The first term in the exponential arises from the rubber-elastic entropic potential for the retractions; the second can be thought of as a softening effect of other relaxations in the entangled environment of the molecule.

If the set of relaxation times over all values of x in eq 1 is taken together with the observation that the relaxation modulus, $G(t)$, is proportional to the square of the number of unrelaxed entanglements, both in ordinary dilution⁶ and for dynamical relaxation,^{4,7,8} then this theory has quantitative predictions for the linear rheology. From the Ball–McLeish model,⁴ $G(t)$ is given by eq 2.

$$G(t) = G_0 \left[\int_0^1 \exp(-t/\tau_{(x)}) dx \right]^2 \quad (2)$$

from which the frequency-dependent dynamic storage and loss moduli, usually observed in rheological experi-

[†] University of Durham.

[‡] University of Leeds.

[®] Abstract published in *Advance ACS Abstracts*, July 15, 1996.

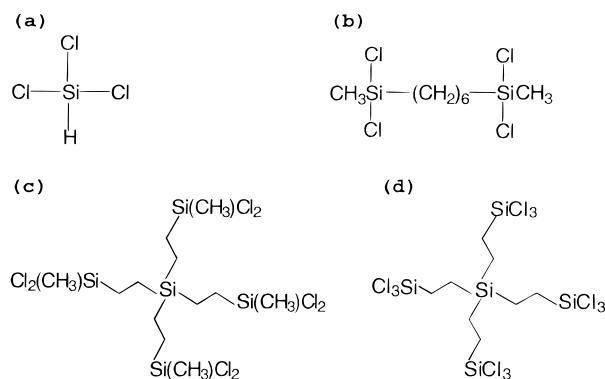


Figure 1. Chemical structures of chlorosilanes used for synthesis of polybutadiene star polymers. (a), (b), (c), and (d) are the cores of the 3-, 4-, 8-, and 12-arm stars, respectively.

ments, may be calculated by the usual one-sided Fourier transform, to give eqs 3a and 3b, respectively.

$$G'(\omega) = G_0 \int_0^1 (1-x) \frac{\omega^2 \tau_{(x)}^2}{1 + \omega^2 \tau_{(x)}^2} dx \quad (3a)$$

$$G''(\omega) = G_0 \int_0^1 (1-x) \frac{\omega \tau_{(x)}}{1 + \omega^2 \tau_{(x)}^2} dx \quad (3b)$$

where G_0 is the plateau modulus.

Experimental Section

Synthesis. The entanglement molecular weight (M_e) of polybutadiene, calculated from literature values⁹ of the plateau modulus, is 1970 g mol⁻¹. For our star polymers, a target arm molecular weight of 30 000 g mol⁻¹ was chosen; therefore each star arm is comprised of approximately 15 entanglement lengths. Star polybutadienes with nominal numbers of arms of 3, 4, 8, and 12 were synthesized, together with a linear polybutadiene (a "2-arm star") of total molecular weight twice that of a star arm.

Precursor arm polybutadiene was prepared¹⁰ by anionic polymerization under high vacuum using benzene as a solvent and *sec*-butyllithium as initiator. After initiation, each reacting solution was stirred overnight at 50 °C, after which time a small sample was collected for molecular weight determination and terminated by addition of degassed methanol.

Four chlorosilanes have been used for this work, as nuclei of the stars, and their chemical formulas are shown in Figure 1.

The tetrafunctional chlorosilane 1,6-bis(dichloromethylsilyl)hexane (Petrarch) was used in the synthesis of the 4-arm star. The octachlorosilane was prepared by the hydrosilation of tetravinylsilane with dichloromethylsilane using chloroplatinic acid as a catalyst according to the procedure of Hadjichristidis et al.¹¹ It should be noted that the hydrosilation of tetravinylsilane gives rise to a mixture of isomers. Although the hydrosilation addition reaction yields mainly the preferred anti-Markovnikov product, if the temperature of the reaction (which is exothermic) is allowed to rise above 40 °C, the degree of Markovnikov addition increases. A dodecachlorosilane was similarly prepared by the hydrosilation of tetravinylsilane with trichlorosilane. Each of the linking agents were diluted with benzene and stored under nitrogen until required.

Star-Branched Polybutadiene Polymers. Construction of the star polymers was achieved by adding the appropriate chlorosilane to the solution of living polybutadiene precursor arm polymer. Each chlorosilane was added as a solution in benzene, and sufficient was added so that there was a 25% mole excess of living polymer to chlorosilane. The solution was then stirred at 50 °C for 3 days before terminating the reaction by adding degassed methanol. The duration of the reaction

time to form star polymers is dependent upon the number of arms. A reaction time of 3 days, while being essential for complete reaction in the formation of 8- and 12-arm stars, is probably excessive for the formation of 3- and 4-arm stars. However, a conservative approach was taken to ensure complete reaction. After termination, the polymer solution was poured into a large excess of methanol to precipitate the polymer. The recovered polymer was dried under vacuum to constant weight before being redissolved in toluene. Methanol was added to this toluene solution held at 25 °C until a precipitate appeared, the quantity of which was less than the total mass of polymer. After redissolving by warming the mixture slightly, it was allowed to cool slowly to 25 °C again. After the precipitated polymer had settled, the supernatant solution, containing unprecipitated star polymer and unreacted linear precursor arm polymer, was removed. The precipitated polymer was then redissolved and the whole fractionation process repeated. Each star polymer was subjected to a total of four precipitations to remove unreacted linear precursor polymer.

Molecular Weight Determination. Molecular weight determination was carried out by size exclusion chromatography (SEC), using both mass and viscosity detectors. It has been shown¹¹ that SEC elution volume for star-branched polymers can show a marked dependence upon the solution concentration. As a result of this, the universal calibration method of obtaining the molecular weight may yield values lower than the true values. To ascertain whether there is a concentration dependence in these cases, polymer solutions at three different concentrations were used for SEC, but over the concentration range used (0.25–0.80 mg cm⁻³), no concentration dependence was evident in the molecular weights obtained. The molecular weights for the stars are shown below in Table 1. The linear "2-arm star" had a M_w of 56 200 and a M_n of 55 440, giving a polydispersity of 1.01.

The functionality of the stars gives an indication of the efficiency of the linking reaction and, in simple terms, tells us the average number of arms per star. The nominal 3-, 4-arm and 12-arm stars have functionality values of 2.8, 3.9, and 11.8, respectively showing that to all intents and purposes the linking reaction has gone to completion. The 8-arm star has a lower than expected functionality of 7.2. This is almost certainly due to an incomplete linking reaction.

We note here that although the fractionation process removed the majority of the unreacted linear polybutadiene precursor polymer, a small quantity always remained in the final star polymer. The amount of unreacted arm present in the star polymer samples was estimated from the areas under the peaks corresponding to the star and linear polymers in the SEC trace, and is given in Table 2.

Thermal Analysis. A Perkin-Elmer DSC7 was used, at a heating rate of 10 °C min⁻¹, and a glass transition temperature of -92 ± 1 °C was obtained for all star polymers and the linear analogue, independent of functionality. No evidence of crystallinity was observed.

Rheology. The dynamic mechanical behavior of the star polymers and the linear analogue was examined on a Rheometrics RDA 2, using parallel-plate geometry, with a dynamic strain amplitude of 0.2%. Frequencies between 0.1 and 100 rad s⁻¹ were employed, over a temperature range from -75 to $+20$ °C, in approximately 10 deg intervals. This temperature and frequency range ensured that, after time-temperature superposition, the entire viscoelastic spectrum from the terminal region (low frequency and high temperature) up to the onset of the Rouse modes and glass transition (high frequency and low temperature) could be observed.

Nuclear Magnetic Resonance. Deuterium NMR measurements were carried out on a 4-arm polybutadiene star sample, where the terminal entanglement length of each star arm was perdeuterated. The procedure for the synthesis of this and other selectively deuterated star polymers will be reported in a separate paper. NMR spectra were recorded at room temperature on a Chemagnetics CMX 200 spectrometer, operating at 30.7 MHz. A standard single-pulse experiment was performed, using a 90° pulse width of 2.75 μs, an

Table 1. Molecular Weights (g mol⁻¹), Polydispersities, and Functionality of Four Polybutadiene Star-Branched Polymers

functionality of chlorosilane	mol wt of linear precursor			mol wt of star polymer ^a			functionality of star ^b
	M_w	M_n	Pd ^c	M_w	M_n	Pd ^c	
3	35 000	34 700	1.01	101 600	98 100	1.036	2.8
4	37 140	37 280	0.996	145 700	145 000	1.005	3.9
8	33 460	33 600	0.996	240 900	239 600	1.006	7.2
12	30 820	30 850	0.999	369 300	363 900	1.015	11.8

^a The molecular weight of the stars is the average value of the molecular weight obtained from three solutions of different concentration.

^b The functionality of the star is the ratio of the $\bar{M}_n(\text{star})/\bar{M}_n(\text{arm})$. ^c Pd is the polydispersity \bar{M}_w/\bar{M}_n .

Table 2. Parameters Obtained from the Fit to the Ball-McLeish Model for Star Polybutadienes and Fraction of Residual Linear Chains Obtained by SEC

functionality	G_0/MPa^a	M_a/M_e^b	$M_e/\text{g mol}^{-1}$	$\tau_0/10^4 \text{ s}^c$	% linear chains
2.0 (linear)	1.0				
2.8	1.1	12.5	2780	0.933	4.3
3.9	1.1	13.5	2760	1.48	7.0
7.2	0.8	10.0	3360	1.66	9.7
11.8	1.0	12.0	2570	1.18	4.5

^a Obtained from inspection of the G' plot. ^b Obtained from best fit to eq 3. ^c At the T_g of -92°C . τ_0 obtained from maximum in G'' , via $\tau_0 = 0.52/\omega_{\text{max}}$.

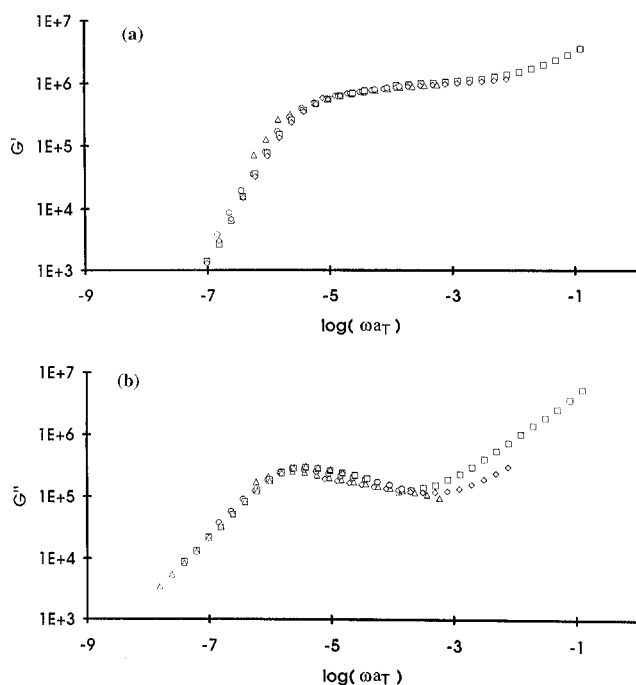


Figure 2. Dynamic shear storage modulus G' (a) and loss modulus G'' (b) for linear polybutadiene of $M_w = 56\,200$ and $M_n = 55\,440$. The different symbols correspond to data acquired at different temperatures prior to time-temperature superposition (see experimental section).

acquisition time of 20 ms, a recycle delay of 15 s, and 2000 acquisitions.

Results and Discussion

Figures 2–6 show the dynamic storage (G') and dynamic loss (G'') modulus versus frequency plots for the linear polymer and the stars. The data at each temperature was shifted horizontally by applying the appropriate WLF shift factors¹² (a_T), using T_g as the reference temperature. Small vertical shift corrections were applied in the usual manner, to account for the temperature change on the modulus due to the rubber-elastic effect, normalizing to 25°C .

To a first approximation, all the star polymers display similar rheological behavior, due to similar arm lengths,

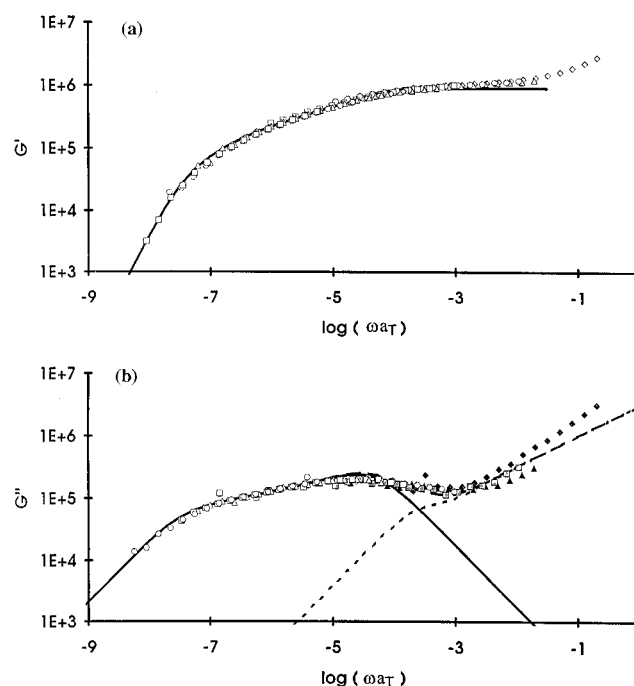


Figure 3. G' (a) and G'' (b) for the 3-arm star. The solid line is the fit to the breathing mode spectrum (eq 3), the dotted line is the fit to the Rouse mode spectrum (eq 9), and the dashed line is the total fit.

and relaxation proceeding via the mechanism discussed in the theoretical section (hereafter referred to as “breathing mode” relaxation) and are significantly different from the linear polymer, which relaxes by means of reptation. The G'' plots in Figures 2b–6b are characteristic of star polymers⁵ and show, at the low-frequency end, the broad spectrum of breathing modes, up to a maximum in G'' at about -4.5 on the log-(frequency) axis. It is this region of the plot that we specifically attempt to model using the present theory. At higher frequencies, the contribution from the Rouse modes is significant and leads to the increase in G'' and G' , which is also due to the approach of the glass transition at the temperatures at which these data sets were acquired. We will demonstrate that the contribution from the Rouse modes can also be modeled, with reasonable success, to provide a theoretical fit to the entire viscoelastic spectrum. The expressions in eqs 3a and 3b were integrated numerically to produce the theoretical breathing mode spectrum for the star polymers, with M_a/M_e being varied to obtain the best fit to the lower frequency end of the data, in each case. The solid lines in Figures 2–6 are examples of such fits with Table 2 giving values for the entanglement molecular weight (M_e) and τ_0 (normalized to T_g) obtained from the fitting procedure, together with the plateau modulus experimentally observed in G' .

The plateau modulus, of about 1 MPa, is similar to the accepted value of 1.15 MPa; however, this is difficult

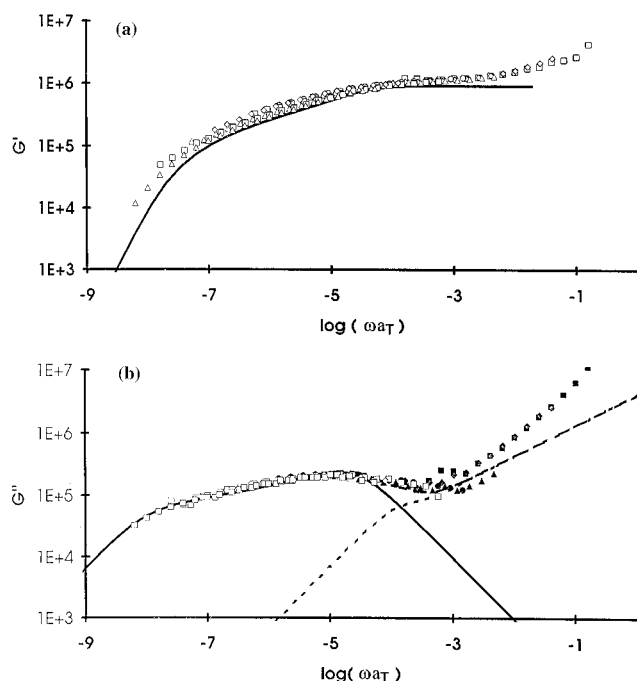


Figure 4. G' (a) and G'' (b) for the 4-arm star. Symbols as for Figure 3.

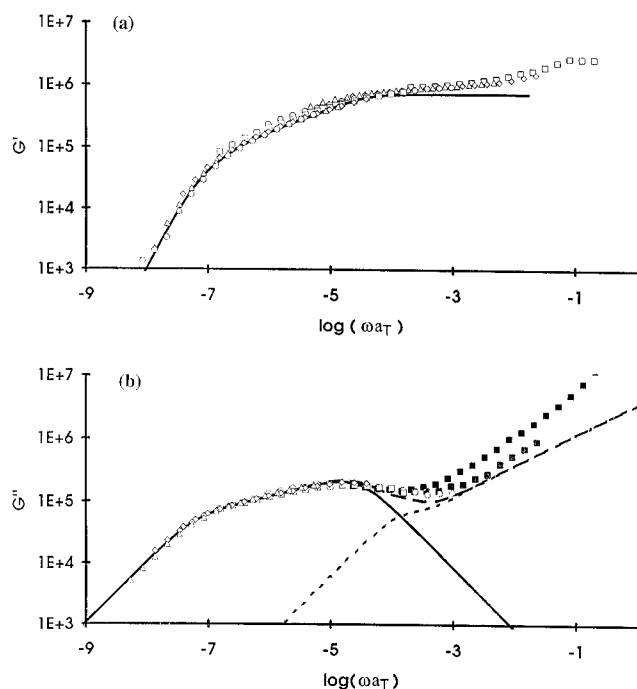


Figure 5. G' (a) and G'' (b) for the 8-arm star. Symbols as for Figure 3.

to measure with any real accuracy as a true plateau is not observed. The theoretical curves (solid lines) for the breathing modes successfully model the low-frequency end of the spectrum in G' and G'' , consistent with the prevalence of entanglement loss up to the peak in $G''(\omega)$. The values for the entanglement molecular weight M_e obtained dynamically, shown in Table 2, are significantly higher than the accepted value⁹ of 1970 g mol⁻¹. We suggest that this phenomenon is explicable in terms of the effect of the free end of the star arm, in the following manner. At long times, relaxed material acts as a solvent for unrelaxed segments nearer the core of the molecule, but even before the retraction-dominated hierarchy of relaxations begins, a significant fraction

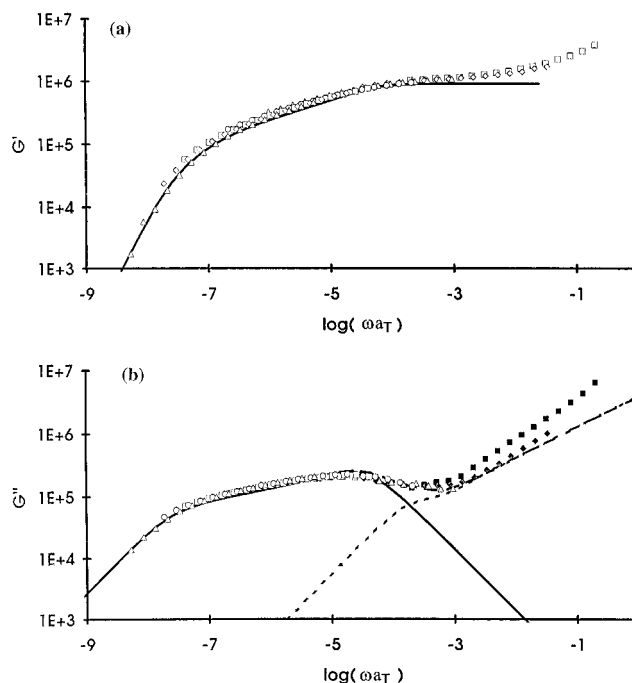


Figure 6. G' (a) and G'' (b) for the 12-arm star. Symbols as for Figure 3.

of entanglements near the end of the free arm may be lost if the free end is undergoing rapid Rouse diffusion along the tube. This will cause rapid loss of all entanglements whose relaxation time is not strongly retarded by the entropic well for path lengths $\tau_{(x)} \approx \tau_{(0)}$, or, alternatively, for those whose entropic barrier to retraction is $\leq kT$. From eq 1, this implies rapid loss of stress from all segments $x \leq x^*$, where x^* is given by

$$\left(\frac{x^{*2}}{2}\right) 2\nu \left(\frac{M_a}{M_e}\right) = 1 \quad (4)$$

and therefore

$$x^* = \left(\frac{M_e}{\nu M_a}\right)^{1/2} \quad (5)$$

The segments within a fraction x^* of the free end should therefore be treated as effective solvent for all times $t < \tau_0$. The consequence of this is that the entanglement molecular weight is predicted to be renormalized to $M_e^* = M_e/(1 - x^*)$. When this modification is applied to the present star polymers, M_e^* becomes about 2400 g mol⁻¹, more similar to the value found from the fits in Table 2.

The foregoing discussion assumes that the terminal entanglement section of the star arm is undergoing Rouse-like dynamics. It is this aspect that can be addressed using NMR. Figure 7 shows the ²H NMR spectrum of a 4-arm star polymer, where the terminal entanglement section has been perdeuterated. The line shape is well described by a sum of two Lorentzians in the ratio 2:1, representing the concentration of methylene and methine deuterons, respectively. The fact that the line shape of the spectrum from each chemically distinct deuteron is Lorentzian confirms that the dynamics of the free end of the star arm are indeed Rouse-like in nature,¹³ supporting the use of the M_e renormalization discussed above. NMR studies of deuterated sections other than the free end will be discussed in much greater detail in a separate paper, but for now

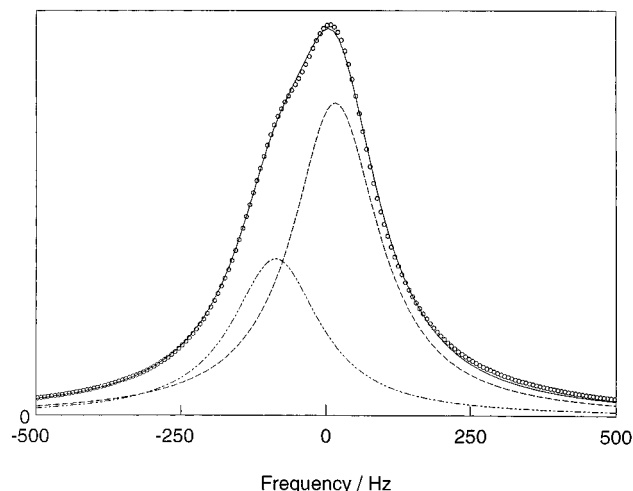


Figure 7. Deuterium NMR spectrum of the terminal entanglement length of a 4-arm star. The solid line is a fit to a sum of two Lorentzians in the ratio 2:1, representing the methylene and methine deuterons. The contribution from each Lorentzian (dashed lines) is also shown.

we state that the spectra of entanglement sections other than the free end are certainly not Lorentzian. The NMR T_2 values for each type of deuteron obtained from the fits in Figure 7 are similar, being 1.77 and 1.73 ms for the methylene and methine, respectively, suggesting that, at a more local level, these microstructural units are undergoing similar dynamics.

Even allowing for the dilution effect of the free end of the star arm, the M_e values obtained are still high. We suggest that this arises because of the small amount of free linear chains left in the samples (see Table 2). To ascertain whether this is a realistic assumption, we need to compare the reptation time for such unreacted star arms, of molecular weight of approximately 30 000 g mol⁻¹ (τ_{r30}), with the attempt time for breathing modes, τ_0 . To calculate τ_{r30} , we can use the data for the linear "2-arm star", of 60 000 g mol⁻¹, (Figure 2b) in the following way. The peak in G' indicates a reptation time for this sample (τ_{r60}) of about 2.5×10^5 s. The reptation time is related¹ to the characteristic Rouse time via eq 6.

$$\tau_{r60} = \frac{3M_{60}}{M_e} \tau_{R60} \quad (6)$$

where τ_{R60} is the Rouse time for the 60 000 MW sample, and M_{60} its molecular weight. The Rouse time for a polymer is proportional to the square of the molecular weight.¹ Therefore, for the unreacted linear chains left in the star polymer samples,

$$\tau_{r30} = \tau_{r60} \left(\frac{M_{30}}{M_{60}} \right)^3 \approx \frac{1}{8} \tau_{r60} \quad (7)$$

where M_{30} is the molecular weight of the free star arm. Hence $\tau_{r30} \approx 3.1 \times 10^4$. This is similar to the values obtained for τ_0 (see Table 2), and hence we might expect these unreacted linear chains to contribute to the entanglement dilution. This is borne out by the last two columns in Table 2, where there is indeed a correlation between τ_0 and the percentage of linear chains left in the samples.

Finally, to provide a complete fit to the data, we need to include the effect on the modulus from the Rouse modes, which will contribute significantly at frequencies

above the maximum in G'' . The essential ingredient is the ratio between the attempt time for breathing relaxations τ_0 and the Rouse time τ_R . The two are closely related because τ_R governs the rate of breathing dynamics; however, τ_0 is slower because, as we have already discussed, entanglements which require an excitation of less than kT in free energy are relaxed typically much faster than the Rouse time of the free arm; it is only retractions which are deeper than $(M_a/M_e)^{1/2}$ which are slowed down by the presence of the tube. For the fastest of these, the elastic free energy is just kT , so we should expect

$$\tau_0 \approx \tau_R e \quad (8)$$

The Rouse spectrum¹ (eq 9) can now be added to the breathing mode spectrum to provide a prediction for the entire frequency range.

$$G'_{\text{Rouse}}(\omega) = G_0 \frac{M_a}{M_e} \sum_{p \text{ odd}}^{\infty} \frac{\omega \tau_p}{1 + \omega^2 \tau_p^2} \quad (9)$$

where $\tau_p = \tau_R/p^2$.

Literature values⁹ of M_e were used, rather than those given in Table 2, as the high-frequency Rouse modes will not be affected by the dilution effect of the free end, as are the breathing modes. Only odd modes are considered as the even modes are suppressed by the branch point.

In each of the Figures 2b–6b, the solid line shows the fit to the breathing mode spectrum (eq 3b), the dotted line to the Rouse spectrum (eq 9), and the dashed line is the sum. In each case, the fit to the low-frequency end is good, but there is a departure between the theory and experiment at high frequency. We consider that this discrepancy is due to the onset of the glass transition. The data sets corresponding to the Rouse region were obtained at -65 to -75 °C, temperatures approaching the glass transition region.

Conclusions

The Ball–McLeish model for the relaxation of star polymer melts has been successfully applied to polybutadiene stars of various functionality. The fits to the theory have resulted in entanglement spacings consistently higher than the accepted value, and this observation has allowed a slight modification to the theory, quantifying a proposed effect of rapid Rouse diffusion of the free end of the star arm, causing entanglement loss. The presence of various small amounts of unreacted residual linear chains in these samples was perhaps serendipitous, since it resulted in an empirical relationship between the concentration of such chains and the attempt time τ_0 for breathing modes, which was attributed to the free chains causing star polymer entanglement dilution via reptation. A simple relationship between τ_0 and the Rouse time has allowed the addition of the high-frequency Rouse mode spectrum. The data shows a departure from the theory in this region, G' increasing at a rate greater than the $\omega^{1/2}$ power law predicted, which can be attributed to the onset of the glass transition.

An underlying feature of the Ball–McLeish model is that the spectrum of relaxation times is related directly to entanglement sections of the star arm, from the penultimate section through to the core. We pursue this

aspect in a separate paper, where we will report on NMR studies of polybutadiene star polymers with specific entanglement sections deuterium labeled.

Acknowledgment. We wish to thank Adrian Kyne for assistance with curve fitting.

References and Notes

- (1) Doi, M.; Edwards, S. F. *The Theory of Polymer Dynamics*; Oxford University Press: Oxford, 1986.
- (2) Doi, M.; Kuzuu, N. Y. *J. Polym. Sci., Polym. Lett. Ed.* **1980**, *18*, 775.
- (3) Pearson, D. S.; Helfand, E. *Macromolecules* **1984**, *17*, 888.
- (4) Ball, R. C.; McLeish, T. C. B. *Macromolecules* **1989**, *22*, 1911.
- (5) Fetters, L. J.; Kiss, A. D.; Pearson, D. S.; Quack, G. F.; Vitus, F. J. *Macromolecules* **1993**, *26*, 647.
- (6) Adam, M.; Fetters, L. J.; Graessley, W. W.; Witten, T. A. *Macromolecules* **1991**, *24*, 2434.
- (7) Des Cloiseaux, J. *Europhys. Lett.* **1988**, *5*, 437.
- (8) O'Connor, N. P. T.; Ball, R. C. *Macromolecules* **1992**, *25*, 5677.
- (9) Fetters, L. J.; Lohse, D. J.; Richter, D.; Witten, T. A.; Zirkel, A. *Macromolecules* **1994**, *27*, 4639.
- (10) Craig, D.; Fowler, R. B. *J. Org. Chem.* **1961**, *26*, 713.
- (11) Hadjichristidis, N.; Guyot, A.; Fetters, L. J. *Macromolecules* **1978**, *11*, 668.
- (12) Ferry, J. D. *Viscoelastic Properties of Polymers*; Wiley: New York, 1980.
- (13) Brereton, M. G. *Macromolecules* **1989**, *22*, 3667.

MA951893W